



LONG-PERIOD GROUND MOTION CHARACTERISTICS IN NIIGATA-KEN CHUETSU AREA, JAPAN, ESTIMATED FROM ACCELERATION DATA OF TELESEISMIC EVENT

T. Uetake⁽¹⁾, K. Hikima⁽²⁾, S. Sekine⁽³⁾, Y. Sawada⁽⁴⁾

⁽¹⁾ Specialist, Tokyo Electric Power Company Holdings Inc., uetake.tomiichi@tepcoco.jp

⁽²⁾ Specialist, Tokyo Electric Power Company Holdings Inc., hikima.kazuhito@tepcoco.jp

⁽³⁾ Researcher, Association for the Development of Earthquake Prediction, ssekine@8f.adep.or.jp

⁽⁴⁾ Director, Association for the Development of Earthquake Prediction, sawada@8f.adep.or.jp

Abstract

In the Niigata-ken Chuetsu area, Japan, there are thick sedimentary layers and long-period ground motions have been observed frequently when large earthquake occurred. There is a high density seismic observation network (AN-net) consisting of 40 stations for studying seismicity in this area. The array size is about 40 km in east-west direction and about 60km in north-south direction. We studied the long-period ground motion characteristics using acceleration data of this array during the 2015 Gorkha, Nepal, earthquake. We detected the low-frequency signals from this teleseismic event in noisy acceleration waveforms and the dominant frequencies of signals were between 0.02 and 0.1 Hz. In such low frequency, the spatial variation of amplitude was recognized in the array area. To emphasize the dominant frequency components, velocity waveforms were made from acceleration waveforms by numerical integration with low-cut filter of 0.02 Hz. Many seismic phases (ex. P-wave, S-wave, Love waves and Rayleigh waves) were clearly recognized in the velocity traces and show the significant characteristics. About the body wave part, the waveforms at the stations in the hill and mountain area were very simple but the large later arrivals were recognized at stations in the plain area. These later arrivals were assumed to be excited by the deep sediment structure in the plain area. About the surface wave part, many wave packets with low frequency were passing through AN-net from the west to the east and the apparent frequency of the wave packets become higher as arrival order of the wave packets. We also confirmed this dispersion characteristics after multiple filtering analysis of the surface wave part data. Next, we estimated the phase velocities and propagation directions of surface waves after the frequency-wavenumber spectrum analysis. The back azimuths were almost between 260 and 280 degree measured clockwise from the north in frequency between 0.02 and 0.1 Hz for both Love and Rayleigh waves. It means that surface waves propagated from the epicenter direction. The estimated phase velocity did not show clear dispersion and did not fit the phase velocity calculated from the existing 1-D velocity model. The sub-surface velocity structure of this area are varied in short distance. The complex velocity structure makes wave propagation complicated. To estimate the phase velocity correctly, it is necessary to use a small array dependent on the local variance of velocity structure.

Keywords: Long-period ground motion; Teleseismic event; Seismic array; Surface wave



1. Introduction

In the Niigata-ken Chuetsu area, Japan, there are thick sedimentary layers and long-period ground motions were observed frequently when large earthquake occurred. A high density seismic observation network (AN-net) consisting of 40 stations has established after the Niigata-ken Chuetsu-oki Earthquake in 2007 for studying of seismicity in this area [1]. We think that this array data is useful to study not only seismicity but also the long-period ground motion characteristics in this area. Since large earthquake generates long-period seismic wave, it is advantage to use large event data for the study of long-period ground motion characteristics. Although large event is rare in local, we try to analyze teleseismic large event data in this study. Generally acceleration data are usually not used in teleseismic event study for its high noise level, but we used the acceleration data in this study.

We analyzed the acceleration records during the Mw7.9 2015 Gorkha Nepal earthquake that occurred about 5,000 km remote from AN-net. The strong motion data recorded in hypocenter area provide an important information for the study of structural damage and seismic source characteristics [2, 3]. The teleseismic data observed in worldwide are also used for realizing the source image [3] but it is not popular to be used studying the local site effects. We think that the teleseismic large event data have several merit for studying the local site factors: The body wave part and surface wave part are completely separate in time domain: The back azimuth from the array stations are almost the same: The records contain long-period components.

2. Location of the event and observation network

The epicenter of the 2015 Gorkha, Nepal, earthquake and location of AN-net are shown in Fig.1 (a). The array configuration of AN-net is shown in Fig.1 (b). AN-net consists of 40 stations deployed in the Niigata-ken Chuetsu area, Japan and its size is about 40 km in east-west direction and 60km in north-south direction. The Gorkha event occurred about 5,000 km remote from AN-net. The back azimuths of epicenter from every station are almost the same. Two feed-back type accelerometers with full scale of $3,920 \text{ cm/s}^2$ are installed at 1.5 m and 100 m in depth and the data are continuously recorded with 100 Hz sampling and 24 bit resolution. The records of the sensors installed 1.5 m in depth were used in this study.

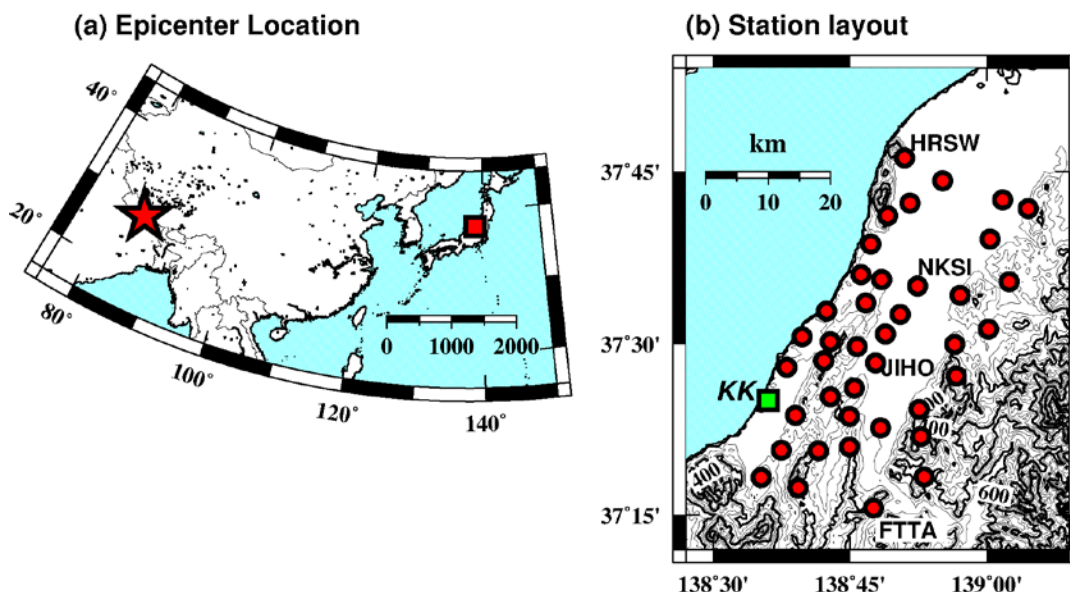
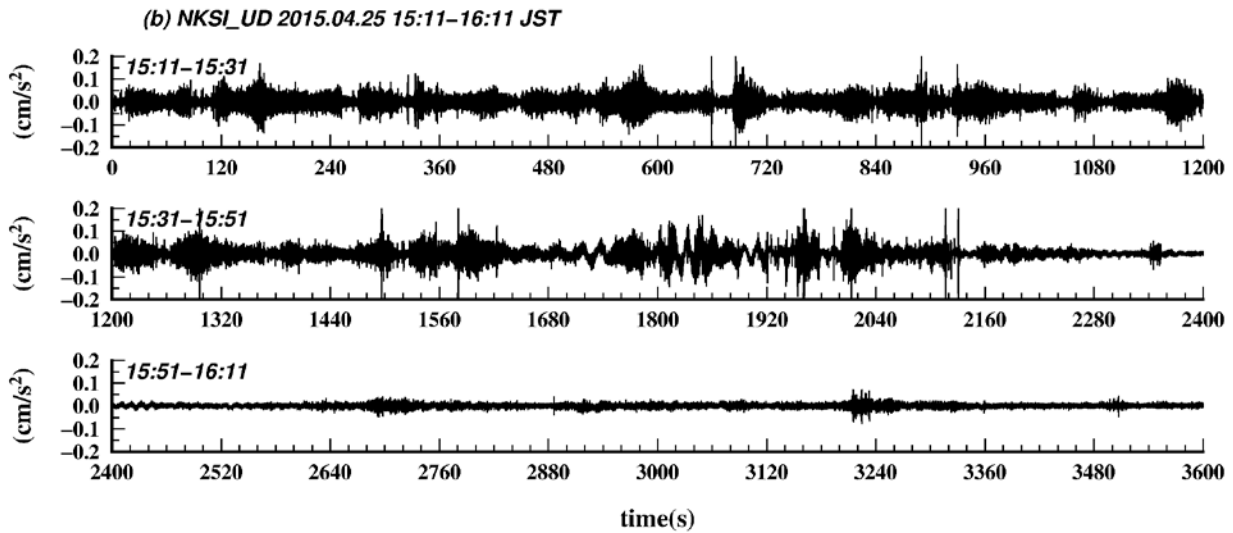




Fig. 1 – Location of epicenter and AN-net. The star and the square in left figure indicate the epicenter of the 2015 Gorkha Nepal earthquake and location of AN-net respectively. Red circles in right figure indicate the AN-net stations and green square indicates the Kashiwazaki-Kariwa nuclear power station.

3. Observed acceleration data

The acceleration records of up-down (UD) component at FTTA and NKSI from 2015.04.25 15:11 to 16:11 in Japan Standard Time (JST) are shown in Fig.2. FTTA is located at the south end of AN-net and in the hill-part. NKSI is located in the center of plain part. The acceleration record at FTTA (Fig.2 (a)) is very low-noise except for several temporary high-frequency waves. Therefore the many phases from the 2015 Gorkha Nepal earthquake can be recognized in this acceleration traces. For examples, the P waves are recognized at about 540 s and the long-period surface waves recognized at 1,650 s or later. In addition, the signals about 1,550 s are the waves from a small deep earthquake occurred in Japan (32.967N, 140.547E, H=81.2km, M5.1). Judging from magnitude and hypocenter depth, the long-period surface waves was not excited by this event. Therefore long-period waves after about 1,650 s are assumed to be the surface waves from the Gorkha earthquake. Different from traces of FTTA, the traces of NKSI (Fig.2 (b)) is very noisy. Many signals in traces of FTTA are covered by noises in traces of NKSI. Only long period waves in the surface wave part are detected at about 1,720 s, 1,820 s and 1,900 s in the traces by comparing with the traces of FTTA.



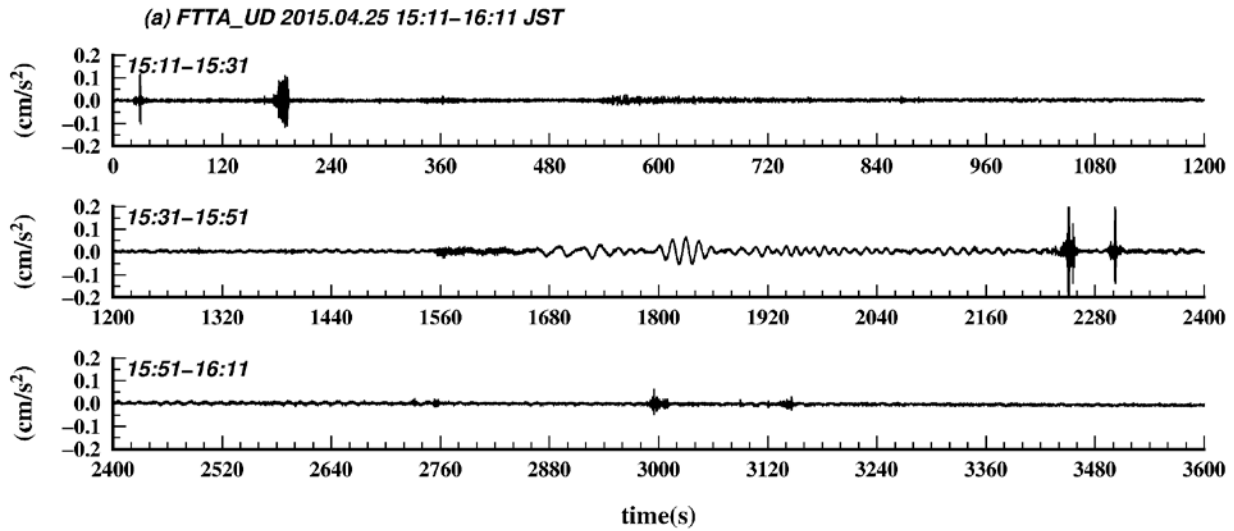


Fig. 2 – Acceleration records of UD component at FTTA and NKSI.

The Fourier spectra of the acceleration records at four stations (HRSW, NKSI, JIHO and FTTA) are shown in Fig.3. Red, green and blue lines indicate North-South (NS), East-West (EW) and UD components respectively. These spectra are made from acceleration waveforms with duration of 3,600 s by FFT method and smoothed by Parzen window of 0.01 Hz. The Location of these stations are shown in Fig.1 (b). HRSW is located at the north end of AN-net and at the foot of Kakuda Mountain. JIHO is located in plain area between FTTA and NKSI. The Fourier Spectra of these stations show almost common characteristics that the amplitude is large in the frequencies between 0.02 and 0.1 Hz and there are two high peaks at 0.05 Hz and 0.08 Hz. The peak amplitude of NKSI at 0.08Hz is almost double of other stations. The spectral amplitude in the high frequency than 1.0 Hz at JIHO and NKSI are larger than that at FTTA and HRSW. In addition, the differences between UD amplitude of UD and amplitude of NS and EW at JIHO and NKSI are also larger than those of FTTA and HRSW. These differences are assumed to be effect of geological condition.

Fig.3 suggests that the spectral amplitude in such a low frequency range is also varied in the array area. To study the spatial variation of Fourier spectral amplitude, we make the spectral ratio with reference to FTTA and plotted the values in the map. Fig.4 (a) and (b) show the results of UD-component and NS-component respectively. The amplitude of UD-component at frequency of 0.0332 Hz is almost the same in AN-net. The amplitude of UD-component at frequency of 0.0500 Hz becomes larger from the south to the north. The amplitude of UD-component at frequency of 0.1001 Hz shows the peak in the north-west side of the AN-net. The amplitude of NS-component at frequency of 0.0332 Hz is almost the same in AN-net. The amplitude of NS-component at frequency of 0.0500 Hz shows peak at the north center of the array. The amplitude of NS-component at frequency of 0.1001 Hz is small in the east and west side of hill and mountain part and large at plain area stations. The amplitude distribution of both components become more complex in higher frequency and the spatial variation of horizontal component are appeared in lower frequency than that of UD-component.

4. Velocity waveform

To avoid the high frequency noises in the acceleration waveforms and to emphasize the dominant frequency components, the velocity waveforms were made from the acceleration traces by numerical integration with low-cut filter of 0.02 Hz in reference to a shape of the acceleration Fourier spectrum. The velocity waveforms at FTTA and NKSI are shown in Fig.5. The top three traces are three components of velocities at NKSI and bottom three traces are those at FTTA. The high frequency noises are suppressed and the seismic signals from the 2015 Gorkha Nepal earthquake can be recognized in the traces at both stations.



The many phases of seismic waves from the first onset of P-wave to the long-period surface wave are recognized in one hour velocity traces. Judging from the geometrical relation with the epicenter and stations, NS-component and EW-component are close to transverse and radial component respectively. The waves detected from 500 to 600 s of traces are P-waves. The waves detected in horizontal component at about 1,000 s of traces are S-waves. The large wave packet detected in NS-component from about 1,250 s is assumed to be Love waves. The large packet detected in EW- and UD-components from about 1,500 s are assumed to be Rayleigh waves. The shape pattern of waveforms at NKSI resembles to those of FTTA but as for the later arrivals of the surface waves at NKSI is more complicated than those of FTTA.

The P wave part in UD-component from 15:19 to 15:21 JST and the S-wave part in NS-component from 15:26 to 15:28 JST are shown in Fig.6. The body wave part propagates through the earth interior and incident to the observation stations almost vertically. As so, we think that the difference of waveforms show the site effects directly. Relatively short period waves overlapped only in P-wave part but the onset of P-wave and S-wave show almost the same motion with period of approximately 20 s. High frequency seismic wave are decreased in a long-distance propagation of the earth interior but it may be a clue to know the property of the source fault motions. In addition, the later arrivals of the S wave part at NKSI are more remarkable than those at FTTA. The later arrivals of S-waves are also remarkable at other stations in plain area. These later arrivals are assumed to be excited by sub-surface structure of the sites.

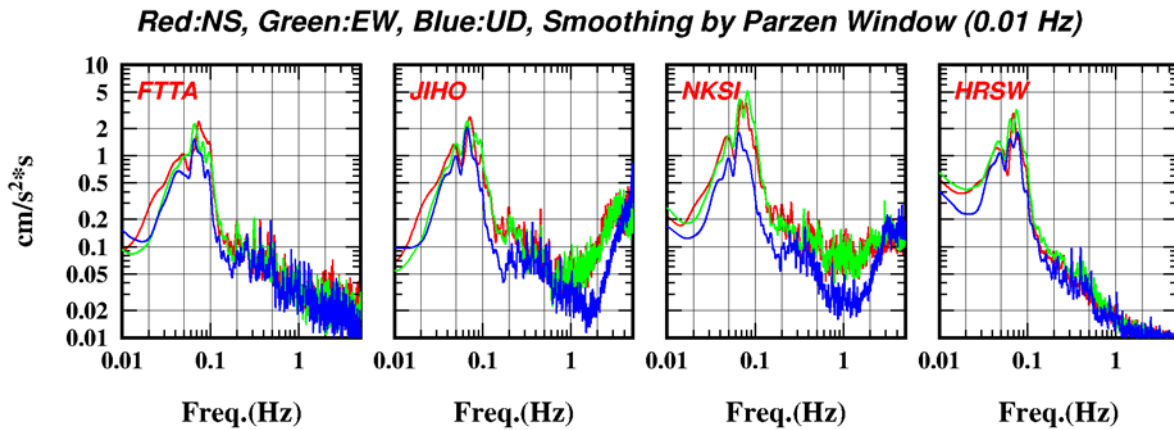


Fig. 3 – Acceleration Fourier spectra of three components. Red, green and blue lines indicate NS-, EW- and UD-components, respectively. Station code is shown as red character and the locations are shown in Fig.1 (b).

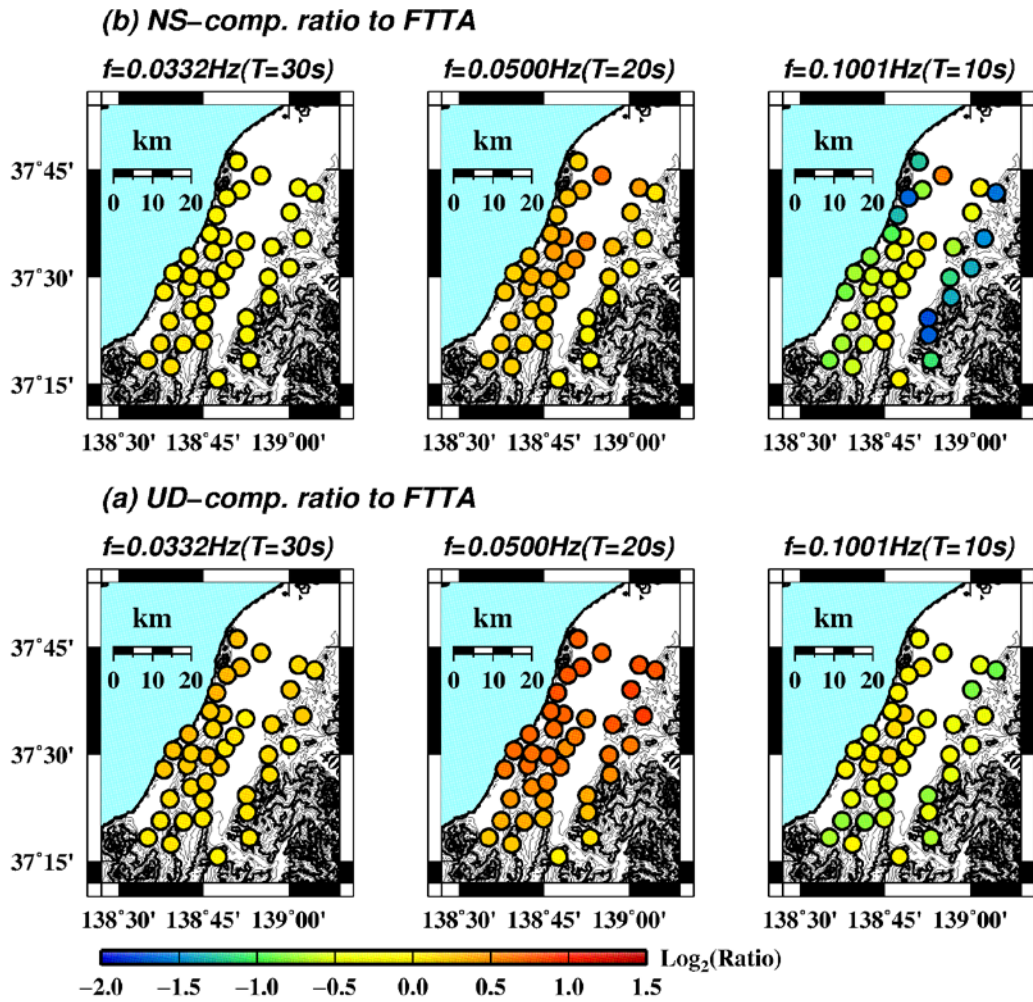


Fig. 4 – Spatial variation of Fourier spectral ratio in reference to FTTA.

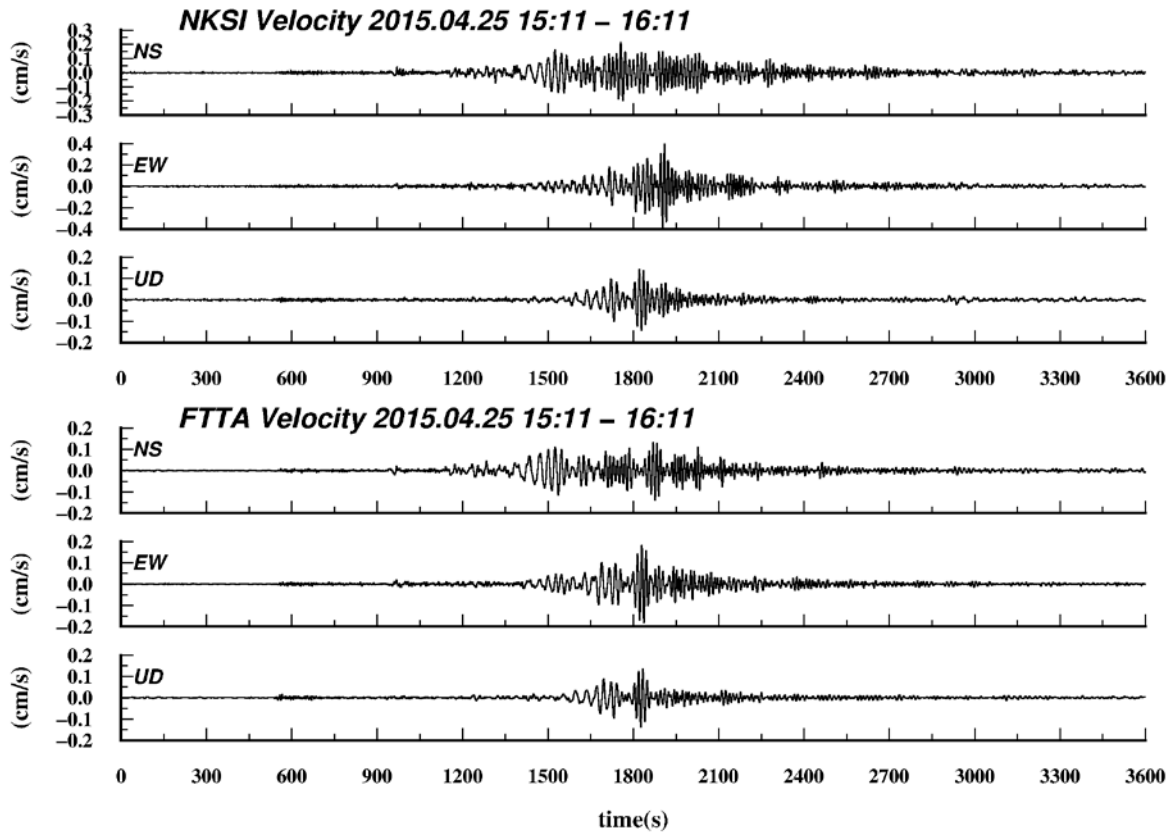


Fig. 5 – Velocity traces at NKSI and FTTA

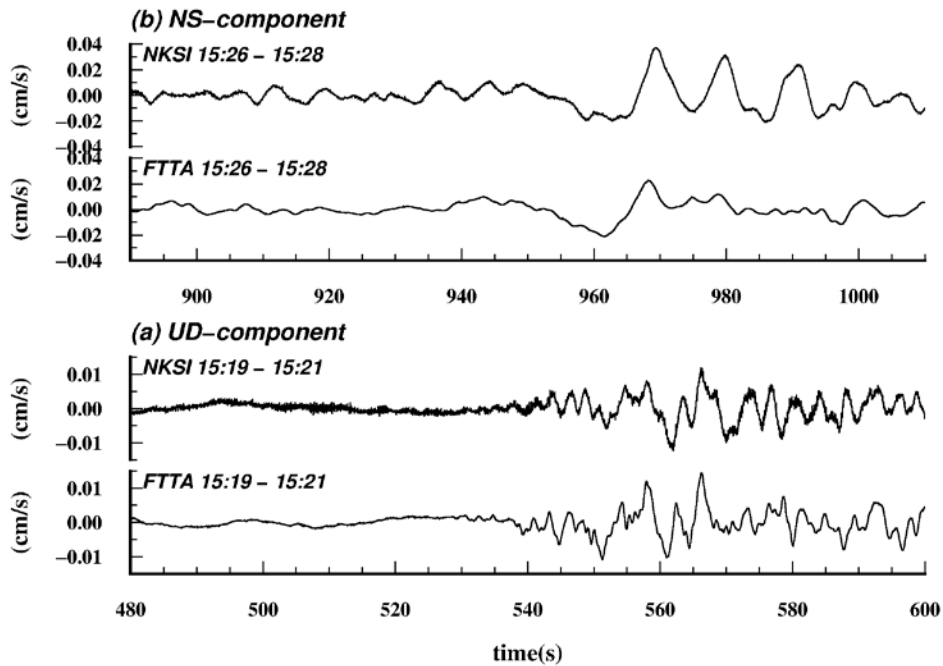


Fig. 6 – Zoom-up of P-wave part and S-wave part in the velocity traces.

5. Surface wave dispersion characteristics

The paste-up of the surface wave part to the east-west section are shown in Fig.7. The left side figure shows the Rayleigh wave part of UD-component from 15:36 to 15:46 JST (from 1,500 s to 2,100 s in Fig.4) and the right side figure shows the Love wave part of NS-component from 15:33 to 15:43 JST (from 1,320 s to 1,920 s in Fig.4). As for the distance in vertical axis is measured along the east-west direction line and zero point is location of HRSW. The left side figure shows that many wave packets in UD-component are passing from the west to the east through AN-net area. In this figure, three lines were drawn on the peaks or troughs of significant wave packets and these lines mean apparent velocities of 4.0 km/s, 3.8 km/s and 3.6 km/s. The apparent velocity of wave packets become slower as arrival order of the wave packets. It provably shows the dispersion characteristics of Rayleigh waves. The wave packets before 360 s in horizontal axis show almost same amplitude and the peak and trough are propagate in phase. As for the wave packet after 360 s, amplitude are variant and the peak and trough are not in phase in the array. The right side figure shows the several wave packets in NS-component are passing from the west to the east, too. In this figure, two lines were drawn on the peak of significant wave packets and those apparent velocities are 4.0 km/s and 3.8 km/s. The change of apparent velocity also shows the dispersion characteristics of Love waves. As for the wave packet after about 300 s, amplitude are variant and the peak and trough are not in phase. The different characteristics of left figure and right figure suggests that the variation of local velocity structure is more effective to Love waves than Rayleigh waves.

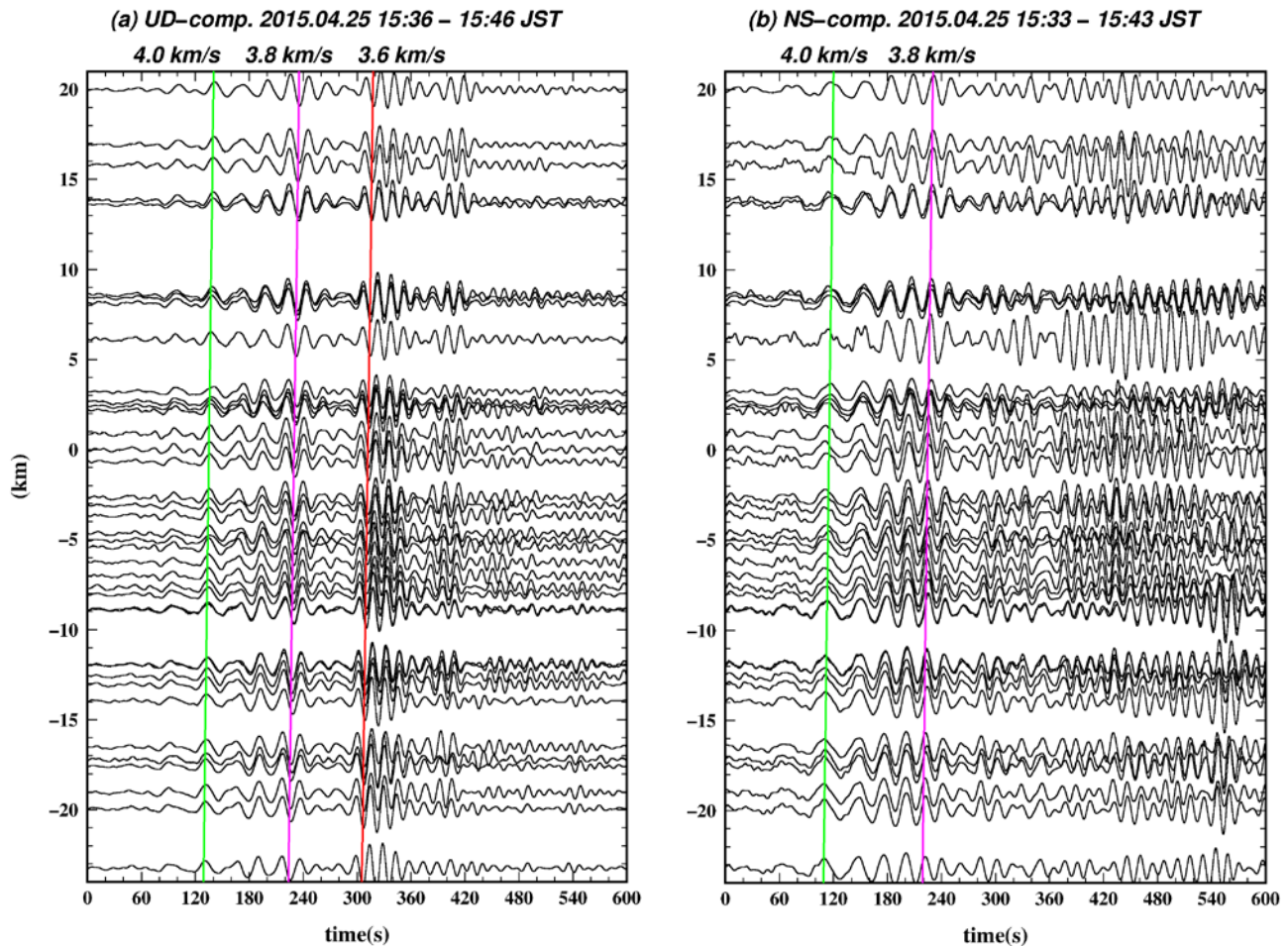


Fig. 7 – Velocity waveforms of surface wave parts.

To evaluate the change of predominant frequency in velocity waveforms along the time axis, we perform the multiple filter analysis [4] for Rayleigh wave part of UD-component and Love wave part of NS-component. The results of UD- and NS-component at FTTA and NKSI are shown in Fig.8. The time windows are selected the same in Fig.7. The predominant frequency turns into 0.1 Hz from 0.02Hz continuously with progress of the time. The dispersion characteristics are different between UD- and NS-component but show similar feature in the traces at FTTA and NKSI. Although, the amplitude of frequency over 0.1 Hz at NKSI are larger than those at FTTA especially in NS-component. This difference between NKSI and FTTA makes different characteristics in later arrivals of Love waves.

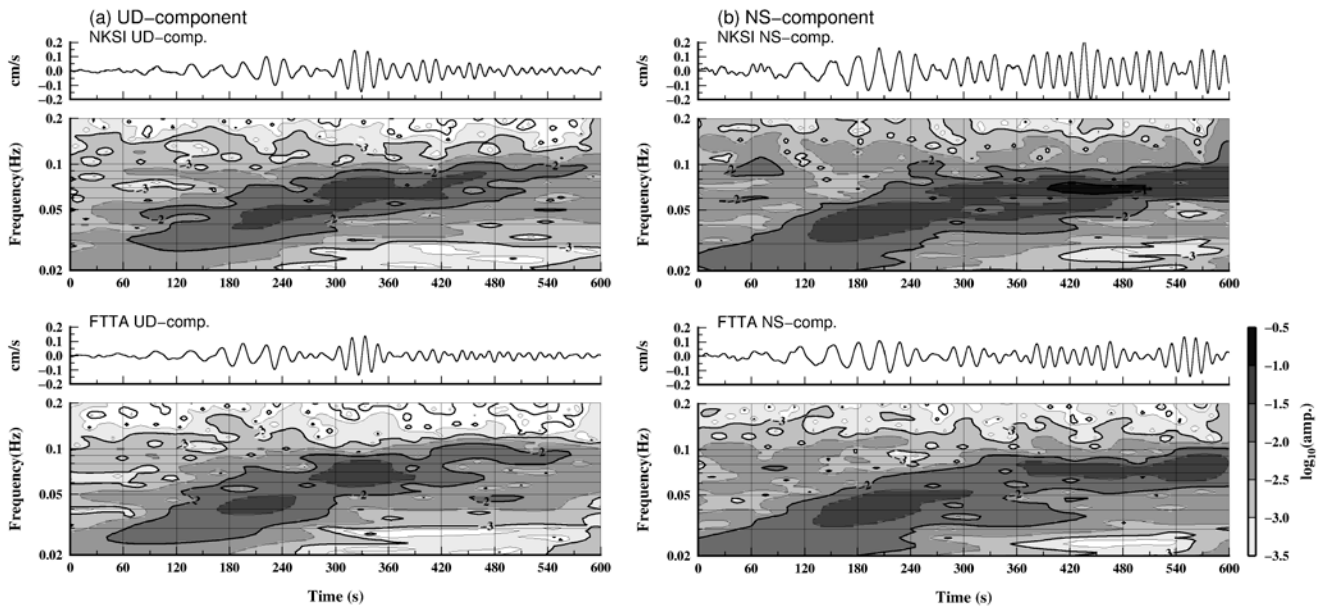


Fig. 8 – Results of multiple filtering analysis for the surface wave parts at FTTA and NKSI.

Since the group delay time as shown in Fig.8 means the integrated value from the epicenter to the observation station along the ray path on the earth surface, it is difficult to evaluate the local velocity structure from this group dispersion characteristics. Therefore we estimated the phase velocity in the array area with applying the frequency-wavenumber spectrum analysis [5] to the surface wave part data. In this study, we used all stations of AN-net to evaluate average phase velocity in this area. The phase velocity evaluated from UD- and NS-component are shown in Fig.9 (a) and (b), respectively. Gray circles indicate phase velocity evaluated in this study. Although Group delay time shows clear dispersion as shown in Fig.8, the phase velocity does not show clear dispersion. About the back azimuth, the values are almost between 260 and 280 degree measured clockwise from the north in frequency between 0.02 to 0.1 Hz. It means that the surface waves propagate from the west and it is coincident with geographical relation of epicenter and AN-net.

The lines show the phase velocity of Rayleigh and Love waves calculated from 1-D velocity structure model of NKSI after the Headquarter for Earthquake Research Promotion (2012) [6]. The velocity model is shown in Table 1. This model has very thick Low velocity surface layers. The lines in left figure are velocity of Rayleigh waves and the lines in right figure are velocity of Love waves. Bold and broken lines indicate the fundamental mode and first higher mode, respectively. The estimated phase velocity do not fit the calculated velocity of fundamental and first higher mode. Small squares in Fig.9 (a) show the phase velocity evaluated from the data of the 2011 off the Pacific coast of Tohoku earthquake using small array consisted of NKSI and other 5 neighborhood stations [7]. Small squares show clear dispersion between 0.05 and 0.1 Hz unlike results in this study.



About the geological structure in Niigata-ken Chuetsu area, it is well known that the deep bedrock, many faults and fold structures. The velocity structure is provably varied in short distance. The variation of spectrum amplitude as shown in Fig.4 and the excitation of later arrivals as shown in Figs. 6 and 7 confirm the variation of velocity structures. To estimate the phase velocity correctly, it is necessary to use a small array dependent on the local variance of velocity structure.

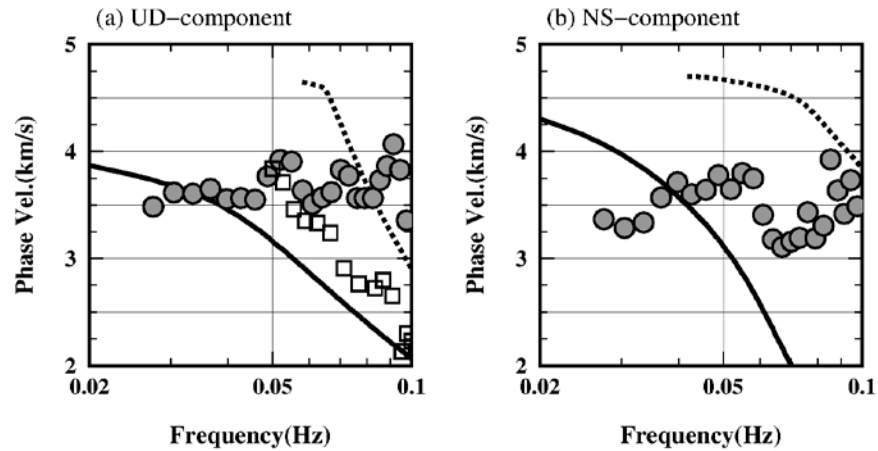


Fig. 9 – Phase velocities evaluated from the surface wave part after frequency-wavenumber spectrum analysis. Gray circle indicates the phase velocity evaluated in this study. Small square indicates the phase velocities after Uetake et al. (2016) [7]. Bold and dotted line indicate the phase velocity calculated from model of Table 1.

Table 1 – Sub-surface velocity structure model for NKSI.

Layer No.	Vp (km/s)	Vs (km/s)	Dens. (kg/m ³)	Thick. (km)
1	2.0	0.6	2.00	0.97
2	2.4	1.0	2.15	0.87
3	2.7	1.3	2.20	1.12
4	3.0	1.5	2.25	0.61
5	3.2	1.7	2.30	1.08
6	3.5	2.0	2.35	0.93
7	5.0	2.9	2.60	1.61
8	5.8	3.4	2.70	8.85
9	6.4	3.8	2.80	13.66
10	7.5	4.5	3.20	88.45
11	8.0	4.7	3.20	-

6. Conclusion

We analyzed the acceleration record of the 2015 Gorkha, Nepal earthquake provided by the dense seismometer array in the Niigata-ken Chuetsu area, Japan. We confirmed the low-frequency signals in noisy acceleration data and the dominant frequencies of the signals are between 0.02 and 0.1 Hz. In such low-frequency, the spatial



distribution of spectrum amplitude vary as frequency and the spatial variance of horizontal component are larger than that of UD-component.

The velocity waveforms were made from the acceleration traces to emphasize low frequency signals and many phases (ex. P-wave, S-wave, Love waves and Rayleigh waves) were clearly recognized in velocity traces. In body wave part, the waveform at hill part stations was simple but the later arrivals were recognized at the plain side station. In surface wave part, many wave packets with low frequency are passing from the west to the east and the apparent velocity of wave packets becomes slower as arrival order. The predominant frequency turns from 0.02 to 0.1 Hz continuously with progress of the time and Rayleigh and Love waves show different dispersion characteristics.

We estimated the phase velocity with applying the frequency-wavenumber spectrum analysis to the surface wave part. The back azimuths were almost between 260 and 290 degree in frequency between 0.02 to 0.1 Hz. It means that surface waves propagate from the west that coincident with geographical relation of the epicenter and AN-net. The estimated phase velocity does not show clear dispersion and did not fit the phase velocity calculated from the existing 1-D velocity model.

About the geological structure in Niigata-ken Chuetsu area, it is well known that the deep bedrock, many faults and fold structures. The velocity structure is provably varied in short distance. The variation of spectrum amplitude and the excitation of later arrivals confirm the variation of velocity structures. To estimate the phase velocity correctly, it is necessary to use a small array dependent on the local variance of velocity structure.

7. Acknowledgements

All figures were drawn with the Generic Mapping Tools (GMT) developed by Wessel and Smith (1998) [8].

8. References

- [1] Sawada Y, Sasaki S, Sekine S, Abe S, Tazawa Y, Sagiya T (2012): Dense seismic and GPS observation around the Nagaoka Plain Western Margin Fault Zone. *15th World Conference of Earthquake Engineering*, Lisbon, Portugal, No.2694.
- [2] Takai N, Shigefuji M, Rajaure S, Bijukchhen S, Ichiyanagi M, Dhital MR, Sasatani T (2016): Strong ground motion in the Kathmandu Valley during the 2015 Gorkha, Nepal, earthquake. *Earth, Planets and Space*, 68:10. DOI: 10.1186/s40623-016-0383-7.
- [3] Kobayashi H, Koketsu K, Miyake H, Takai N, Shigefuji M, Bhattarai M, Sapkota SN (2016): Joint inversion of teleseismic, geodetic, and near-field waveform datasets for rupture process of the 2015 Gorkha, Nepal, earthquake. *Earth, Planets and Space*, 68:66. DOI: 10.1186/s40623-016-0441-1.
- [4] Dziewonski A, Bloch S, Landisman M (1969): A technique for the analysis of transient seismic signals. *Bull. Seism. Soc. Am.*, Vol.59, pp.427-444.
- [5] Capon J (1969): High resolution frequency-wavenumber spectrum analysis. *Proceedings of IEEE*, 57, 1408-1418.
- [6] Headquarter for Earthquake Research Promotion (2012): Subsurface velocity structure model used in the Long-period strong ground motion prediction map, 2012 trial version.
(http://www.jishin.go.jp/evaluation/seismic_hazard_map/lpshm/12_choshuki_dat/)
- [7] Uetake T, Hikima K, Sekine S, Sawada Y (2016): Spatial variation of ground motion of Niigata-ken Chuetsu Area during the 2011 off the Pacific coast of Tohoku earthquake - Analysis of the Data from Dense Observation Array -. *Journal of Japan Association for Earthquake Engineering*, Vol.16, No.4, P.4_66-4_79 (in Japanese with English abstract).
- [8] Wessel P and Smith WHF (1998): New, improved version of the Generic Mapping Tools released. *Eos Trans. AGU*, 79, 579.